

Modified Wavelet Method for Solving Two-dimensional Coupled System of Evolution Equations

Inderdeep Singh^{a*}, Sheo Kumar^b

^aDepartment of Physical Sciences, Sant Baba Bhag Singh University,
Jalandhar-144030, Punjab, India

^bDepartment of Mathematics, Dr. B.R.Ambedkar National Institute of
Technology, Jalandhar-144011, Punjab, India

E-mail: inderdeeps.ma.12@gmail.com

E-mail: sheoks53@gmail.com

ABSTRACT. As two-dimensional coupled system of nonlinear partial differential equations does not give enough smooth solutions, when approximated by linear, quadratic and cubic polynomials and gives poor convergence or no convergence. In such cases, approximation by zero degree polynomials like Haar wavelets (continuous functions with finite jumps) are most suitable and reliable. Therefore, modified numerical method based on Taylor series expansion and Haar wavelets is presented for solving coupled system of nonlinear partial differential equations. Efficiency and accuracy of the proposed method is depicted by comparing with classical methods.

Keywords: Haar wavelet, Taylor series, Collocation points, Nonlinear coupled evolution equations, Operational matrices.

2000 Mathematics subject classification: 65N99.

*Corresponding Author

Received 19 September 2018; Accepted 11 December 2020
©2022 Academic Center for Education, Culture and Research TMU

1. INTRODUCTION

A system of nonlinear PDEs play a significant role in nonlinear physical science because they provide much physical information and more insight into the physical aspects of the problem and thus lead to further applications such as fluid mechanics, plasma physics, physical chemistry, biology, solid state physics, chemical kinematics and geochemistry. The motivation of this paper is to extend the analysis of the Haar wavelet collocation method to solve three different kinds of nonlinear coupled equations, namely, the $(2 + 1)$ -dimensional coupled system of breaking soliton equations ([3], [12], [14]), Whitham-Broer-Kaup wave equations for dispersive long waves in the shallow water [1] and the variant Boussinesq equations [13].

During 19th century, wavelets were used in many applications of research and technology. Haar wavelet being discontinuous and non-differentiable, is the oldest mathematical tool for solving linear as well as nonlinear PDEs. It is used for solving differential and integral equations in many research papers such as [2], [6], [11], [15], [16], [17], [20], [21] and [22]. Efficient approaches are presented in [4], [5], [8] and [9] for solving nonlinear PDEs.

The rest of this paper is arranged as follow:

In Section 2, we simply provide the mathematical framework of the computational operational matrices based on Haar wavelet basis functions. In Section 3, in order to illustrate the method, three models arising in physics are investigated. Convergence of Haar wavelet method is discussed in Section 4 and convergence of quasilinearisation technique is presented in Section 5. In Section 6, numerical examples are solved to establish the efficiency and accuracy of the present method by comparing the numerical results with Adomain decomposition method (ADM) and finite difference method (FDM). Stability of the proposed method is discussed in Section 6. Finally, some conclusion and discussion are provided.

2. HAAR WAVELET

Haar functions are orthogonal family of switched rectangular waveforms where amplitudes can differ from one function to another. These are defined in $[\alpha_1, \alpha_3]$ as below:

$$H_i(x) = \begin{cases} 1, & \alpha_1 \leq x < \alpha_2, \\ -1, & \alpha_2 \leq x < \alpha_3, \\ 0, & \text{elsewhere,} \end{cases} \quad (2.1)$$

where $\alpha_1 = \frac{k}{m}$, $\alpha_2 = \frac{k+0.5}{m}$ and $\alpha_3 = \frac{k+1}{m}$. Integer $m = 2^j$, ($j = 0, 1, 2, 3, 4, \dots, J$) indicates the level of the wavelet, and $k = 0, 1, 2, 3, \dots, m - 1$ is the translation

parameter. Maximal level of resolution is J . The index $i = m + k + 1$. In case of minimal values, $m = 1$, $k = 0$ we have $i = 2$. The maximal value of i is $i = 2M$, where $M = 2^J$.

Define the collocation points $x_l = \frac{(l-0.5)}{2M}$, where $l = 1, 2, 3, \dots, 2M$. The operational matrix of integration, which is a $2M \times 2M$ square matrix, is defined by the relations:

$$P_{1,i}(x) = \begin{cases} x - \alpha_1, & x \in [\alpha_1, \beta_1), \\ \gamma_1 - x, & x \in [\beta_1, \gamma_1), \\ 0, & \text{elsewhere,} \end{cases} \quad (2.2)$$

and

$$P_{2,i}(x) = \begin{cases} \frac{1}{2}(x - \alpha_1)^2, & x \in [\alpha_1, \beta_1), \\ \frac{1}{4m^2} - \frac{1}{2}(\gamma_1 - x)^2, & x \in [\beta_1, \gamma_1), \\ \frac{1}{4m^2}, & x \in [\gamma_1, 1), \\ 0, & \text{elsewhere.} \end{cases} \quad (2.3)$$

3. APPLICATIONS

In this section, the modified Haar wavelet collocation method is used to find the approximate solutions of three kinds of coupled evolution equations, namely, $(2 + 1)$ - dimensional coupled system of breaking soliton equations, Whitham-Broer-Kaup wave equations for dispersive long waves in the shallow water and the variant Boussinesq equations. The system of partial differential equations is converted into a system of nonlinear ordinary differential equations by using some wave transformations and apply quasilinearisation technique to convert a system of nonlinear ordinary differential equations into a system of linear ordinary differential equations and then apply Haar wavelet collocation method to solve such linear system of ordinary differential equations. All the equations discussed in this paper have non-linear phrases of power type.

3.1 $(2 + 1)$ - dimensional system of breaking soliton equations described in [12]:

$(2 + 1)$ - dimensional interaction of a Riemann wave propagating along the y -axis with a long wave along the x -axis is represented as

$$\begin{cases} u_t + au_{xxy} + 4auv_x + 4au_xv = 0, \\ u_y = v_x, \end{cases} \quad (3.1)$$

where a is known constant.

Using wave variable transformation

$$\begin{cases} u(x, y, t) = u(\xi), \\ v(x, y, t) = v(\xi), \quad \xi = x + y - \eta t. \end{cases} \quad (3.2)$$

From (3.1), we obtain

$$\begin{cases} -\eta u'(\xi) + au'''(\xi) + 4au(\xi)v'(\xi) + 4au'(\xi)v(\xi) = 0, \\ u'(\xi) = v'(\xi). \end{cases} \quad (3.3)$$

Integrating the second equation of (3.3) with respect to ξ , and for simplicity, considering the constants of integration equal to zero, we obtain

$$u(\xi) = v(\xi). \quad (3.4)$$

Substituting (3.4) into first equation of (3.3) and integrating one time, we obtain

$$-\eta u(\xi) + 4au^2(\xi) + au''(\xi) = 0. \quad (3.5)$$

After simplification, from (3.5), we obtain

$$au''(\xi) = \eta u(\xi) - 4au^2(\xi), \quad (3.6)$$

with initial conditions obtained from exact solutions. The exact solutions of (3.6) are finding by using tanh-coth method combined with Riccati equation as discussed in [3] and [14]. Choosing the initial value approximation say $u_0(\xi)$. Comparing the Equation (3.6) with

$$u''(\xi) = F(\xi, u(\xi), u'(\xi)). \quad (3.7)$$

We have $F(\xi, u(\xi), u'(\xi)) = \frac{1}{a}[\eta u(\xi) - 4au^2(\xi)]$. Expanding the nonlinear function F around the initial approximation $u_0(\xi)$, using Taylor series up to two terms, to linearize the nonlinear term. From (3.7), we obtain

$$\begin{aligned} u''(\xi) = F[u'_0(\xi), u_0(\xi), \xi] + [u(\xi) - u_0(\xi)] \frac{dF}{du_0} [u'_0(\xi), u_0(\xi), \xi] \\ + [u'(\xi) - u'_0(\xi)] \frac{dF}{du'_0} [u'_0(\xi), u_0(\xi), \xi]. \end{aligned} \quad (3.8)$$

Applying (3.8) in (3.6), we obtain

$$au''(\xi) = [\eta u_0(\xi) - 4au_0^2(\xi)] + (u(\xi) - u_0(\xi))(\eta - 8au_0(\xi)). \quad (3.9)$$

After simplification, from (3.9), we obtain

$$au''(\xi) - (\eta - 8u_0(\xi))u(\xi) = 4au_0^2(\xi). \quad (3.10)$$

Consider the Haar wavelet approximation

$$u''(\xi) = \sum_{i=1}^{2M} a_i \mathcal{H}_i(\xi), \quad (3.11)$$

and integrating (3.11), twice with respect to ξ , from 0 to ξ , we obtain

$$u'(\xi) = u'(0) + \sum_{i=1}^{2M} a_i \mathcal{P}_{1,i}(\xi), \quad (3.12)$$

and

$$u(\xi) = u(0) + \xi u'(0) + \sum_{i=1}^{2M} a_i \mathcal{P}_{2,i}(\xi). \quad (3.13)$$

From (3.10), (3.11), (3.12) and (3.13), we obtain the system of algebraic equations. After solving such system of algebraic equations, we obtain wavelet coefficients. The approximate solution of (3.9), say $u_1(\xi)$ is obtained by substituting the wavelet coefficients into (3.13). Repeating the above procedure for $u_1(\xi)$, we obtain approximate solution say $u_2(\xi)$. The accuracy of the approximate solution is increases by repeating the above process. To illustrate the efficiency and accuracy, these approximation results are compared with exact solutions given in [3] and [14]. These solutions were obtained with the aid of tanh-coth method combined with Riccati equations.

3.2 Whitham-Broer-Kaup model:

Whitham-Broer-Kaup model for dispersive long waves in the shallow water small-amplitude regime is given by

$$\begin{cases} u_t + uu_x + v_x + bu_{xx} = 0, \\ v_t - (uv)_x - bv_{xx} + cu_{xxx} = 0, \end{cases} \quad (3.14)$$

where $u = u(x, t)$ is the field of horizontal velocity, $v = v(x, t)$ is the height that deviates from the equilibrium position of the liquid and b, c are constants which are represented in different diffusion powers. Using the wave variable transformation $u(x, t) = u(\xi)$ and $v(x, t) = v(\xi)$, $\xi = x - \delta t$, the system of partial differential equations is converted into the following system of ordinary differential equation

$$\begin{cases} -\delta u' + uu' + v' + bu'' = 0, \\ -\delta v' + (uv)' - bv'' + cu''' = 0. \end{cases} \quad (3.15)$$

Solving the first equation of (3.15) for the function $v = v(\xi)$, we obtain the relation

$$v = \delta u - \frac{1}{2}u^2 - bu'. \quad (3.16)$$

Substituting (3.16) in the second equation of (3.15), we obtain the following ordinary differential equation

$$(b^2 + c)u'' - \frac{1}{2}u^3 + \frac{3}{2}u^2 - \delta^2 u = 0. \quad (3.17)$$

The exact solutions of (3.17) are finding by using $\frac{G'}{G}$ expansion method as discussed in [1].

Comparing the Equation (3.17) with

$$u''(\xi) = F(\xi, u(\xi), u'(\xi)), \quad (3.18)$$

where F is a nonlinear function in term of u and u' . The value of F in this case is $F(\xi, u(\xi), u'(\xi)) = \frac{1}{(b^2+c)} \left[\delta^2 u(\xi) - \frac{3}{2} u^2(\xi) + \frac{1}{2} u^3 \right]$. Expanding the nonlinear function F around initial approximation say $u_0(\xi)$, using Taylor series up to two terms, to linearize the nonlinear term. From (3.18), we obtain

$$u''(\xi) = F[u'_0(\xi), u_0(\xi), \xi] + [u(\xi) - u_0(\xi)] \frac{dF}{du_0} [u'_0(\xi), u_0(\xi), \xi] + [u'(\xi) - u'_0(\xi)] \frac{dF}{du'_0} [u'_0(\xi), u_0(\xi), \xi]. \quad (3.19)$$

Applying (3.19) in (3.18), we obtain

$$(b^2 + c)u''(\xi) = \left[\frac{1}{2}u_0^3 - \frac{3}{2}u_0^2 + \delta^2 u_0 \right] + (u(\xi) - u_0(\xi)) \left(\frac{3}{2}u_0^2 - 3u_0 + \delta^2 \right). \quad (3.20)$$

After simplification, from (3.20), we obtain

$$(b^2 + c)u''(\xi) - \left(\frac{3}{2}u_0^2 - 3u_0 + \delta^2 \right) = -u_0^3 + \frac{3}{2}u_0^2. \quad (3.21)$$

Consider the Haar wavelet approximation

$$u''(\xi) = \sum_{i=1}^{2M} a_i \mathcal{H}_i(\xi), \quad (3.22)$$

and integrating (3.22), twice with respect to ξ , from 0 to ξ , we obtain

$$u'(\xi) = u'(0) + \sum_{i=1}^{2M} a_i \mathcal{P}_{1,i}(\xi), \quad (3.23)$$

and

$$u(\xi) = u(0) + \xi u'(0) + \sum_{i=1}^{2M} a_i \mathcal{P}_{2,i}(\xi). \quad (3.24)$$

From (3.21), (3.22), (3.23) and (3.24), we obtain the system of algebraic equations. After solving such system of algebraic equations, we obtain wavelet coefficients. The approximate solution of (3.20), say $u_1(\xi)$ is obtained by substituting the wavelet coefficients into (3.24). Repeating the above procedure for $u_1(\xi)$, we obtain approximate solution say $u_2(\xi)$. The accuracy of the approximate solution is increases by repeating the above process. By substituting the values of $u(x, t)$ into (3.16), we obtain solution $v(x, t)$. To illustrate the efficiency and accuracy of the proposed method, these approximate solutions are compared with exact solutions given in [1] and are given by

$$u(x, t) = \frac{\delta(A + B) \left(1 + \tanh \left(\frac{\delta(x - \delta t)}{2\sqrt{b^2 + c}} \right) \right)}{\left(B + A \tanh \left(\frac{\delta(x - \delta t)}{2\sqrt{b^2 + c}} \right) \right)}, \quad (3.25)$$

provided $A \neq \pm B$, where A , B and δ are free parameters. Accordingly the solution of $v(x, t)$ is

$$v(x, t) = \frac{1}{2\sqrt{b^2 + c}} \frac{\delta^2(A + B)^2(\sqrt{b^2 + c} - b)}{\left(B \cosh\left(\frac{\delta(x - \delta t)}{2\sqrt{b^2 + c}}\right) + A \sinh\left(\frac{\delta(x - \delta t)}{2\sqrt{b^2 + c}}\right)\right)^2} \quad (3.26)$$

3.3 The Variant Boussinesq Equations:

In this section, we will apply the modified Haar wavelet method to find the approximate solution of the variant Boussinesq equation in the form

$$\begin{cases} u_t + H_x + uu_x = 0, \\ H_t + (uH)_x + u_{xxx} = 0. \end{cases} \quad (3.27)$$

Using the wave variable transformation $u(x, t) = u(\xi)$ and $H(x, t) = H(\xi)$, $\xi = x - \omega t$, the system of partial differential equations is converted into the following system of ordinary differential equation

$$\begin{cases} -\omega u' + H' + uu' = 0, \\ -\omega H' + (uH)' + u''' = 0. \end{cases} \quad (3.28)$$

Solving the first equation of (3.28) for the function $H = H(\xi)$, we obtain the relation

$$H = \omega u - \frac{1}{2}u^2. \quad (3.29)$$

Substituting (3.29) in the second equation of (3.28), we obtain the following ordinary differential equation

$$u'' - \frac{1}{2}u^3 + \frac{3}{2}\omega u^2 - \omega^2 u = 0. \quad (3.30)$$

The exact solutions of (3.28) are finding by using MSE method as discussed in [13]. Consider the initial approximation is $u_0(\xi)$. After using the proposed method, we obtain

$$u''(\xi) - (1 - 3u_0 + \frac{3}{2}u_0^2)u_{r+1} = -u_0^3 + \frac{3}{2}u_0^2. \quad (3.31)$$

From (3.31), (3.22), (3.23) and (3.24), we obtain the system of algebraic equations. After solving such system of algebraic equations, we obtain wavelet coefficients. The approximate solution of (3.31), say $u_1(\xi)$ is obtained by substituting the wavelet coefficients into (3.24). Repeating the above procedure for $u_1(\xi)$, we obtain approximate solution say $u_2(\xi)$. The accuracy of the approximate solution is increases by repeating the above process. By substituting the values of $u(x, t)$ into (3.29), we obtain solution $H(x, t)$. To illustrate the efficiency and accuracy of the proposed method, these approximate solutions are compared with exact solutions given in [13] and are given by

$$u(x, t) = \omega \left(1 \pm \tanh\left(\frac{\omega}{2}(x - \omega t)\right)\right), \quad (3.32)$$

and

$$H(x, t) = \frac{\omega^2}{2} \operatorname{sech}^2 \left(\frac{\omega}{2} (x - \omega t) \right). \quad (3.33)$$

4. CONVERGENCE OF HAAR WAVELET METHOD

The convergence of Haar wavelet method, given in [2] is stated below:

Assume that $u(\xi)$ be a differentiable function with bounded first order derivative on $[0, 1]$ and $u_{2M}(\xi)$ be the Haar wavelet approximation solution. Then, the error function is

$$\text{error} = \| u(\xi) - u_{2M}(\xi) \| \leq \frac{1}{2^J}. \quad (4.1)$$

From (3.18), we see that error is inversely proportional to the level of resolution. It ensures the convergence of Haar wavelet approximation at higher level of resolution J .

5. CONVERGENCE OF QUASILINEARIZATION TECHNIQUE

Consider the nonlinear second order differential equation

$$y''(x) = F(y), \quad (5.1)$$

with initial conditions

$$y(0) = y(b) = 0. \quad (5.2)$$

Using quasilinearization technique, from (5.1), we obtain

$$y''_{r+1}(x) = F(y_r) + [y_{r+1}(x) - y_r(x)]F'(y_r), \quad (5.3)$$

with initial conditions

$$y_{r+1}(0) = y_{r+1}(b) = 0. \quad (5.4)$$

Let $y_0(x)$ be some initial approximation. Each function $y_{r+1}(x)$ is a solution of a (5.3), where y_r is always considered known and is obtained from the previous iteration. Now, subtracting r th equation from the $(r+1)$ th equation, we obtain

$$[y_{r+1} - y_r]'' = f(y_r) - f(y_{r-1}) + [y_{r+1} - y_r]f'(y_r) - [y_r - y_{r-1}]f'(y_{r-1}). \quad (5.5)$$

Considering (5.5) as a differential equation for $[y_{r+1} - y_r]$ and converting (5.5) into an integral equation, we obtain

$$[y_{r+1} - y_r] = \int_0^b K(x, y) \left[F(y_r) - F(y_{r-1}) + [y_{r+1} - y_r]F'(y_r) - [y_r - y_{r-1}]F'(y_{r-1}) \right] dy, \quad (5.6)$$

where $K(x, y)$ is a Green's function and is given by

$$K(x, y) = \begin{cases} \frac{x(y-b)}{b}, & 0 \leq x < y \leq b, \\ \frac{(x-b)y}{b}, & b \geq x > y \geq 0. \end{cases} \quad (5.7)$$

It is observed that $\max_{x,y} |K(x, y)| = \frac{b}{4}$, where maximisation is taken over the region $0 \leq x < y \leq b$. Now, by using Taylor's series, we obtain

$$F(y_r) = F(y_{r-1}) + [y_r - y_{r-1}]F'(y_{r-1}) + \frac{[y_r - y_{r-1}]^2}{2}F''(u), \quad y_{r-1} < u < y_r. \quad (5.8)$$

Consider $\max_y (|F(y)|, |F'(y)|) = m < \infty$ and $\max_u (F''(u)) = k$. From (5.6), we obtain

$$| [y_{r+1} - y_r] | \leq \int_0^b |K(x, y)| \left[| [y_{r+1} - y_r] | |F'(y_r)| + \frac{[y_r - y_{r-1}]^2}{2} |F''(u)| \right] dy. \quad (5.9)$$

Taking maximization of (5.9), over x , we obtain

$$\max_x | [y_{r+1} - y_r] | \leq \frac{b}{4} \int_0^b \left[\max_x | [y_{r+1} - y_r] | m + \max_x \frac{[y_r - y_{r-1}]^2}{2} k \right] dy. \quad (5.10)$$

After simplification, from (5.10), we obtain

$$\max_x | [y_{r+1} - y_r] | \leq \frac{b^2 m}{4} \max_x | [y_{r+1} - y_r] | + \frac{b^2 k}{8} \max_x [y_r - y_{r-1}]^2. \quad (5.11)$$

After simplification, from (5.11), we obtain

$$\max_x | [y_{r+1} - y_r] | \leq \frac{\frac{b^2 k}{4}}{1 - \frac{b^2 m}{4}} \max_x [y_r - y_{r-1}]^2. \quad (5.12)$$

Thus, the convergence is quadratic in nature.

6. NUMERICAL EXPERIMENTS AND DISCUSSION

To illustrate the accuracy and efficiency of the proposed method, some numerical examples are solved using proposed method. The obtained numerical results are compared with exact solutions. We also report L_∞ , L_2 and RMS errors of the computed solutions which are defined as

$$L_\infty(u) = \max_{1 \leq i \leq 2M} |u_{Exact}(\xi_i) - u_{Approximate}(\xi_i)|, \quad (6.1)$$

$$L_2(u) = \sqrt{\sum_{i=1}^{2M} [|u_{Exact}(\xi_i) - u_{Approximate}(\xi_i)|]^2}, \quad (6.2)$$

and

$$RMS = \sqrt{\frac{\sum_{i=1}^{2M} [|u_{Exact}(\xi_i) - u_{Approximate}(\xi_i)|]^2}{2M}}. \quad (6.3)$$

The method with far less degrees of freedom and with smaller CPU time provides better solutions than classical ones. Among all the wavelet families mathematically most simple are the Haar wavelets. We introduce a Haar wavelet method for solving two-dimensional coupled systems because it has many advantages features:

- Very high accuracy and fast transformation and possibility of implementation of fast algorithms compared with other known methods.
- The simplicity and the small computational costs resulting from the sparsity of the transform matrices and the small number of significant wavelet coefficients.
- Haar wavelet method is also very convenient for solving two-dimensional boundary value problems, as the boundary conditions are taken care of automatically.

Example 1.

For Equation (3.1), letting $\eta = a = 1$, the exact solution of (3.10) is

$$u(x, y, t) = v(x, y, t) = \frac{3}{8} \sec h^2 \left(\frac{x + y - t}{2} \right). \quad (6.4)$$

Table 1 shows the comparison of different norms of errors of Example 1 for third iteration at different values of J . Table 2 show the comparison of Haar wavelet solution (Third iteration and $J=9$) with exact solution, FDM and ADM (Three-term approximation) at $t = 0.1$. Table 3 shows the computational time of each method used in Example 1. Figure 1 shows the comparison of solutions $u(\xi)$ and $v(\xi)$ of Example 1 for third iteration for $J = 4$. Figure 2 shows the comparison of absolute errors of Example 1 for third iteration at $J = 4$. Figure 3 and Figure 4 shows the physical behavior of solutions of Example 1 at $t = 1/32$ and $t = 31/32$ respectively.

Example 2.

For Equation (3.1), letting $\eta = 4a$ and $a = 1$, the exact solutions of (3.10), is given by

$$u(x, y, t) = v(x, y, t) = \frac{3}{2} \sec h^2(x + y - 4t). \quad (6.5)$$

Table 4 shows the comparison of different norms of errors of Example 2 for third iteration at different values of J . Table 5 show the comparison of Haar wavelet solution (Third iteration and $J=9$) with exact solution, FDM and ADM at $t = 0.025$. Table 6 shows the computational time of each method used in

J	2M	$L_\infty(\xi)$	$L_2(\xi)$	RMS error
1	4	2.7026E-004	4.4369E-004	2.2185E-004
2	8	6.2056E-005	1.0861E-004	3.8399E-005
3	16	1.6099E-005	2.7448E-005	6.8621E-006
4	32	4.1201E-006	6.8883E-006	1.2177E-006

TABLE 1. Comparison of errors of Example 1 at third iterations for different values of J .

x=y	Exact solution	Haar wavelet solution (J=9)	FDM solution	ADM solution
0.1	0.3740640602	0.3740640603	0.3741000000	0.3740640625
0.2	0.3666874675	0.3666874681	0.3667835408	0.3666890625
0.3	0.3525055683	0.3525055699	0.3526443326	0.3525390625
0.4	0.3325693099	0.3325693127	0.3327340362	0.3328140625
0.5	0.3082504610	0.3082504649	0.3084275266	0.3093140625

TABLE 2. Comparison of solutions of Example 1 at $t = 0.1$.

2M	Comput. time of Haar wavelet method (in sec)	Comput. time of ADM (in sec)	Comput. time of FDM (in sec)
4	0.22	0.27	0.31
8	0.38	0.52	0.55
16	1.59	2.05	2.25
32	7.12	9.57	10.22
64	15.58	19.18	20.12

TABLE 3. Comput. times of different methods of Ex 1.

Example 2. Figure 5 and Figure 6 shows the physical behavior of solutions of Example 2 at $t = 1/32$ and $t = 23/32$ respectively. Figure 7 shows the comparison of solutions $u(\xi)$ and $v(\xi)$ of Example 2 for third iteration for $J = 4$. Figure 8 shows the comparison of absolute errors of Example 2 for third iteration at $J = 4$.

Example 3.

For Equation (3.1), letting $\eta = -4a$ and $a = 1$, the exact solution is

$$u(x, y, t) = v(x, y, t) = \frac{1}{2}[1 - 3\tanh^2(x + y + 4t)]. \tag{6.6}$$

Table 7 shows the comparison of different norms of errors of Example 3 for third iteration at different values of J . Table 8 shows the comparison of Haar wavelet solution (Third iteration and $J=4$) with exact solution and FDM at $t = 0.025$. Table 9 shows the computational time of each method used in

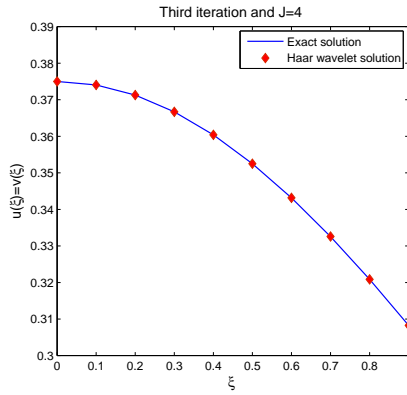


FIGURE 1. Comparison of solutions of Example 1 for third iteration and $J = 4$.

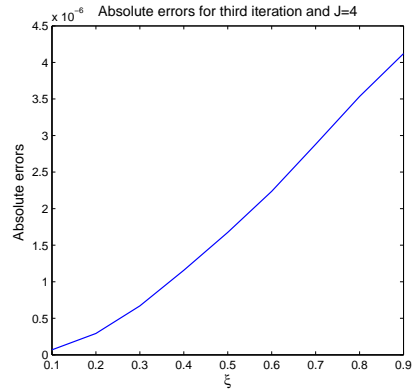


FIGURE 2. Absolute errors of Example 1 for third iteration at $J = 4$.

J	2M	$L_\infty(\xi)$	$L_2(\xi)$	RMS error
1	4	5.7587E-003	1.1613E-002	4.1059E-003
2	8	1.4085E-003	3.0346E-003	1.0729E-003
3	16	3.4106E-004	7.6843E-004	2.7168E-004
4	32	8.7036E-005	1.9274E-004	6.8144E-005

TABLE 4. Comparison of errors of Example 2 at third iterations for different values of J .

x=y	Exact solution	Haar wavelet solution (J=9)	FDM solution	ADM solution
0.1	1.4850994362	1.4850994409	1.4850000000	1.4850994333
0.2	1.3727054427	1.3727054783	1.3719483800	1.3726869000
0.3	1.1796715994	1.1796716707	1.1781602658	1.1786458333
0.4	0.9521093849	0.9521094706	0.9503031742	0.9384322333
0.5	0.7303760417	0.7303761128	0.7288876135	0.6399501000

TABLE 5. Comparison of solutions of Example 2 at $t = 0.025$.

Example 3. Figure 9 show the comparison of solutions of Example 3 for third iteration at $J = 4$ and Figure 10 show the absolute errors of Example 3 for third iteration at $J = 4$.

Example 4:

2M	Comput. time of Haar wavelet method (in sec)	Comput. time of ADM (in sec)	Comput. time of FDM (in sec)
4	0.27	0.28	0.31
8	0.29	0.44	0.56
16	1.49	2.01	2.15
32	4.28	5.22	6.01
64	13.33	18.25	19.12

TABLE 6. Comput. times of different methods of Ex 2.

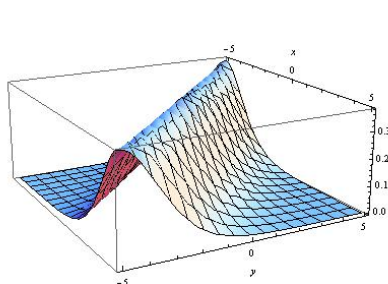


FIGURE 3. Physical behavior of solutions of Example 1 at $t = 1/32$.

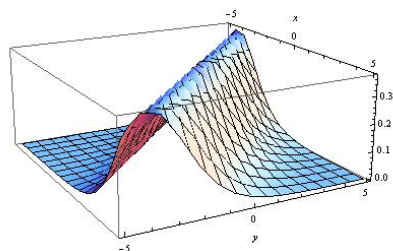


FIGURE 4. Physical behavior of solutions of Example 1 at $t = 31/32$.

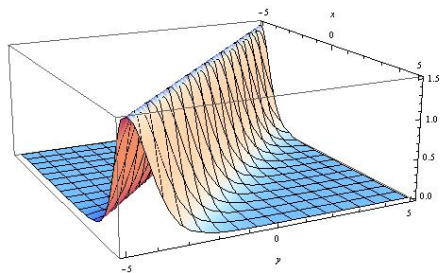


FIGURE 5. Physical behavior of solutions of Example 2 at $t = 1/32$.

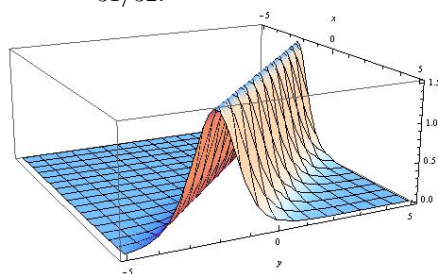


FIGURE 6. Physical behavior of solutions of Example 2 at $t = 23/32$.

In Equation (3.14), take $c = 3, b = 1$ and $\delta = 1$. If $A = 0, B = 1$, the exact solution is

$$u(x, t) = 1 + \tanh\left(\frac{x - t}{4}\right), \tag{6.7}$$

and

$$v(x, t) = \frac{1}{4} \operatorname{sech}^2\left(\frac{x - t}{4}\right). \tag{6.8}$$

Table 10 and Table 11 shows the different norms of errors of Example 4 for solution $u(x, t)$ and $v(x, t)$ for third iteration at different values of J . Table 12

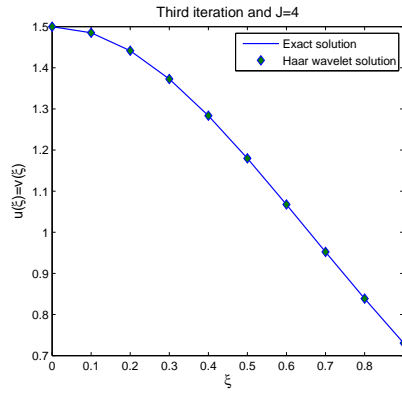


FIGURE 7. Comparison of solutions of Example 2 for third iteration and $J = 4$.

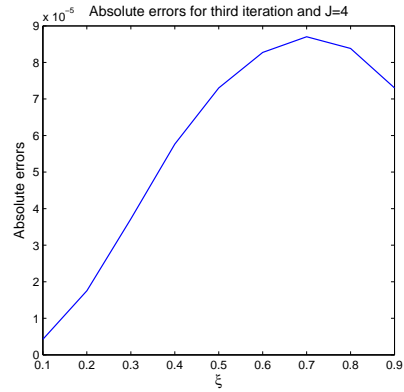


FIGURE 8. Absolute errors of Example 2 for third iteration at $J = 4$.

J	2M	$L_\infty(\xi)$	$L_2(\xi)$	RMS error
1	4	5.7587E-003	1.1613E-002	5.8066E-003
2	8	1.4085E-003	3.0346E-003	1.0729E-003
3	16	3.4106E-004	7.6843E-004	1.9211E-004
4	32	8.7036E-005	1.9274E-004	3.4072E-005

TABLE 7. Comparison of errors of Example 3 at third iterations for different values of J .

x=y	Exact solution	Haar wavelet solution (J=4)	FDM solution
0.05	0.4415644744	0.4415820320	0.4411910000
0.10	0.3727054427	0.3727426501	0.3719483800
0.15	0.2834581791	0.2835158273	0.2822940010
0.20	0.1796715994	0.1797446173	0.1781602658
0.25	0.0673666438	0.0674493873	0.0656304767

TABLE 8. Comparison of solutions of Example 3 at $t = 0.025$.

and Table 13 shows the comparison of Haar wavelet solutions $u(x, t)$ and $v(x, t)$ (Third iteration and $J=4$) with exact solution and FDM. Table 14 shows the computational time of each method used in Example 4. Figure 11 shows the comparison of solution $u(x, t)$ with exact solution for third iteration at $J = 3$. Figure 12 shows the comparison of absolute errors of solution $u(x, t)$ for third

2M	Comput. time of Haar wavelet method (in sec)	Comput. time of FDM (in sec)
4	0.27	0.32
8	0.35	1.12
16	1.52	2.38
32	7.48	8.12
64	15.03	19.24

TABLE 9. Comput. time of different methods of Ex 3.

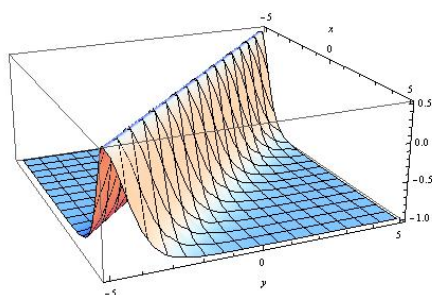


FIGURE 9. Physical behavior of solutions of Example 3 for $-5 \leq x \leq 5$, $-5 \leq y \leq 5$ and $t = 1/32$.

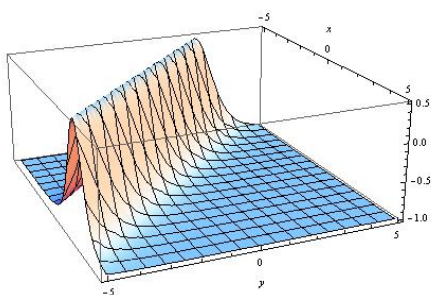


FIGURE 10. Physical behavior of solutions of Example 3 for $-5 \leq x \leq 5$, $-5 \leq y \leq 5$ and $t = 23/32$.

J	2M	$L_\infty(\xi)$	$L_2(\xi)$	RMS
1	4	1.4082E-004	2.6606E-004	1.3303E-004
2	8	3.4459E-005	6.6322E-005	2.3448E-005
3	16	8.6882E-006	1.6616E-005	4.1541E-006
4	32	2.1846E-006	4.1572E-006	7.3489E-007

TABLE 10. Comparison of errors of solution $u(x, t)$ of Example 4 at third iterations for different values of J .

iteration at $J = 3$. Figure 13, Figure 14, Figure 15 and Figure 16 shows the physical behavior of solutions of Example 4 for different x and t .

Example 5:

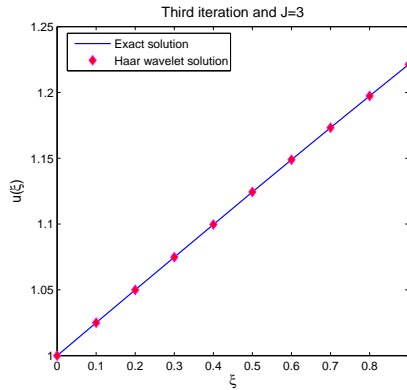


FIGURE 11. Comparison of solution $u(x, t)$ of Example 4 for third iteration and $J = 3$.

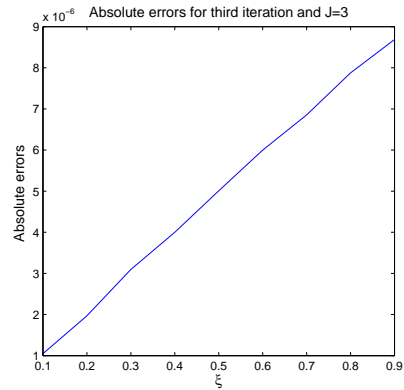


FIGURE 12. Comparison of absolute errors of Example 4 for third iteration at $J = 3$.

J	2M	$L_\infty(\xi)$	$L_2(\xi)$	RMS
1	4	2.3410E-004	5.6391E-004	2.8196E-004
2	8	5.8576E-005	1.4093E-004	4.9828E-005
3	16	1.4647E-005	3.5231E-005	8.8078E-006
4	32	3.6564E-006	8.8174E-006	1.5587E-006

TABLE 11. Comparison of errors of solution $v(x, t)$ of Example 4 at third iterations for different values of J .

x	Exact solution	Haar wavelet solution (J=4)	FDM solution
0.5	1.0249947929	1.0249945464	1.0250000000
0.9	1.0499583749	1.0499578713	1.0499995120
1.3	1.0748596906	1.0748589283	1.0749980499
1.7	1.0996679946	1.0996669801	1.0999951312
2.1	1.1243530017	1.1243517497	1.1249902791

TABLE 12. Comparison of solutions $u(x, t)$ of Example 4 at $t = 0.1$.

In Equation (3.28), take $\omega = 1$. The exact solution is

$$u(x, t) = 1 + \tanh\left(\frac{x - t}{2}\right), \tag{6.9}$$

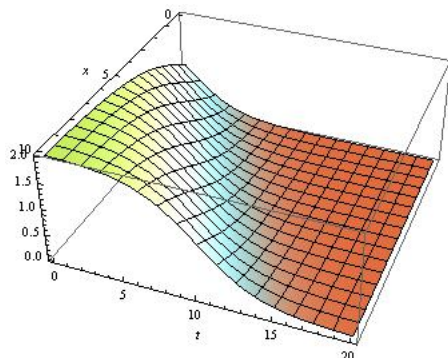


FIGURE 13. Physical behavior of $u(x,t)$ of Example 4 for $0 \leq x \leq 10$ and $0 \leq t \leq 20$.

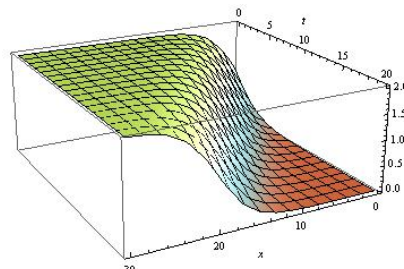


FIGURE 14. Physical behavior of $u(x,t)$ of Example 4 for $0 \leq x \leq 30$ and $0 \leq t \leq 20$.

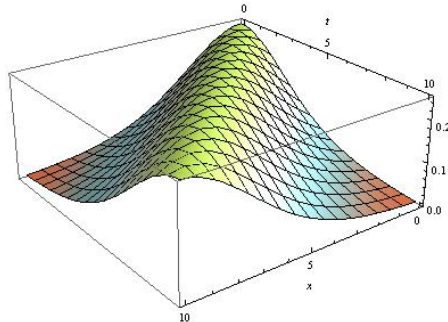


FIGURE 15. Physical behavior of $v(x,t)$ of Example 4 for $0 \leq x \leq 10$ and $0 \leq t \leq 10$.

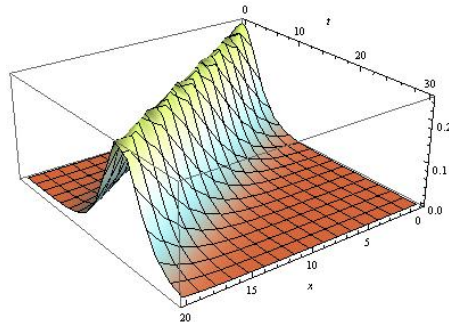


FIGURE 16. Physical behavior of $v(x,t)$ of Example 4 for $0 \leq x \leq 20$ and $0 \leq t \leq 30$.

x	Exact solution	Haar wavelet solution (J=4)	FDM solution
0.5	0.2498438150	0.2498462573	0.2497875000
0.9	0.2493760401	0.2493796965	0.2487549041
1.3	0.2485990066	0.2486026594	0.2472022671
1.7	0.2475165727	0.2475190471	0.2450296734
2.1	0.2461340827	0.2461342776	0.2422372366

TABLE 13. Comparison of solutions $v(x,t)$ of Example 4 at $t = 0.1$.

and

$$H(x,t) = \frac{1}{2} \operatorname{sech}^2\left(\frac{x-t}{2}\right). \tag{6.10}$$

2M	Comput. time of Haar wavelet method (in sec)	Comput. time of FDM (in sec)
4	0.23	0.33
8	0.37	0.44
16	1.19	2.02
32	8.14	8.32
64	14.11	16.10

TABLE 14. Comput. time of different methods of Example 4.

Table 15 and Table 16 show the comparison of numerical solutions $u(x, t)$ and $H(x, t)$ with exact solution and FDM. Table 17 shows the computational time of each method used in Example 5.

ξ	Exact solution	Haar wavelet solution (J=4)	FDM solution
0.1	1.0499583749	1.0499564059	1.0500000000
0.2	1.0996679946	1.0996639956	1.0997506250
0.3	1.1488850336	1.1488790371	1.1490074595
0.4	1.1973753202	1.1973674436	1.1975357990
0.5	1.2449186624	1.2449090881	1.2451149991
0.6	1.2913126124	1.2913014557	1.2915422585
0.7	1.3363755443	1.3363628759	1.3366357074
0.8	1.3799489622	1.3799349146	1.3802367217
0.9	1.4218990052	1.4218837444	1.4222114255

TABLE 15. Comparison of solutions $u(x, t)$ of Example 5 for $\omega = 1$.

7. STABILITY OF PROPOSED METHOD

There are many ways to describe the idea of stability analysis. Clearly a computation is stable if it does not "blow up". In this section, we find the stability of the numerical computations using the procedure based on Patra & Ray (2014). The stability of a numerical computation is calculated by taking the different length step size ω . To obtain a stable result, a set of different length step sizes are considered. The stability criterion in this analysis is related with 1% of the relative error to u_0 for the given simulation time.

$$R.E = \left| \frac{u_{Approximate} - u_0}{u_{Approximate}} \right| \times 100 \leq 1\%, \quad (7.1)$$

where $u_{Approximate}$ is the approximated value of u , which is obtained from our proposed method. To show the behavior of solutions of above examples,

ξ	Exact solution	Haar wavelet solution (J=4)	FDM solution
0.1	0.4987520803	0.4987521787	0.4987500000
0.2	0.4950331454	0.4950335439	0.4950249064
0.3	0.4889166233	0.4889175161	0.4888983884
0.4	0.4805214914	0.4805230460	0.4804898040
0.5	0.4700074244	0.4700097692	0.4699593185
0.6	0.4575684809	0.4575717309	0.4575015557
0.7	0.4434257465	0.4434300078	0.4433382002
0.8	0.4278193930	0.4278247303	0.4277100177
0.9	0.4110006146	0.4110070531	0.4108687560

TABLE 16. Comparison of solutions $H(x, t)$ of Example 5 for $\omega = 1$.

2M	Comput. time of Haar wavelet method (in sec)	Comput. time of FDM (in sec)
4	0.24	0.29
8	0.36	1.14
16	1.54	2.25
32	5.43	6.38
64	13.20	20.14

TABLE 17. Comput. time of different methods of Example 5.

consider the interval $0.125 \leq \omega \leq 0.0009765625$.

For Example 1, take $u_0 = 0.374$, the values of R.E is less than 0.02%.

For Example 2, take $u_0 = 1.48$, the values of R.E is less than 0.3%.

For Example 3, take $u_0 = 0.44$, the values of R.E is less than 0.3%.

For Example 4, take $u_0 = 1.00$, the values of R.E is less than 0.31%.

For Example 5, take $u_0 = 1.04$, the values of R.E is less than 0.9%.

From above numerical computation, we see that all the relative errors are less than 1% for the given interval of ω , which confirm the computational stability of u by our proposed method. Therefore, the proposed method is stable.

8. CONCLUSION

It is concluded that, the proposed Haar wavelet method is computationally simple, numerically fast for solving coupled evolution equations arising in mathematical physics. The approximate solutions tends to exact solutions by increasing level of resolutions and number of iterations. The significant feature of proposed method is that it is applicable for high dimension problems (see, for Example 1). It is easy to handle ordinary differential equations rather than partial differential equations for nonlinear problems. This method with far less degrees of freedom and with smaller CPU time provides solutions with negligible error. For getting the necessary accuracy the number of calculation points may be increased.

ACKNOWLEDGMENT

We are grateful to the anonymous reviewers for their valuable comments which led to the improvement of the manuscript.

REFERENCES

1. M. Alquran, A. Qawasmeh, Soliton Solutions of Shallow Water Wave Equations by Mean of G'/G Expansion Method, *Journal of Applied Analysis and Computation*, **4**(3), (2014), 221–229.
2. E. Babolian, A. Shamsavaran, Numerical Solution of Nonlinear Fredholm Integral Equations of the Second Kind Using Haar Wavelet, *Journal of Computational and Applied Mathematics*, **225**, (2009), 87–95.
3. A. Bekir, A. Cevikel, The Tanh-coth Method Combined with the Riccati Equation for Solving Nonlinear Coupled Equation in Mathematical Physics, *Journal of King Saud University–Science*, **23**, (2011), 127–132.
4. A.H. Bhrawy, An Efficient Jacobi Pseudospectral Approximation for Nonlinear Complex Generalised Zakharov System, *Appl. Math. Comput.*, **247**, (2014), 30–46.
5. A. H. Bhrawy, A Highly Accurate Collocation Algorithm for 1 + 1 and 2 + 1 Fractional Percolation Equations, *J. Vibrat. Control*, **22**, (2016), 2288–2310.
6. I. Celik, Haar Wavelet Method for Solving Generalized Burgers-Huxley Equation, *Arab Journal of Mathematical Sciences*, **18**(1), (2012), 25–37.
7. C. F. Chen, C. H. Hsiao, Haar Wavelet Method for Solving Lumped and Distributed-parameter Systems, *IEE Proc., Control Theory Appl.*, **144**, (1997), 87–94.
8. E. H. Doha, A. H. Bhrawy, A Jacobi Spectral–Galerkin Method for the Integrated Forms of Fourth–order Elliptic Differential Equations, *Num. Methods Par. Diff. Equ.*, **25**, (2009), 712–739.
9. E. H. Doha, A. H. Bhrawy, An Efficient Direct Solver for Multidimensional Elliptic Robin Boundary Value Problems Using a Legendre Spectral–Galerkin Method, *Comp. Math. Appl.*, **64**, (2012), 558–571.
10. A. Haar, Zur Theorie Der Orthogonalen Funktionsysteme, *Math. Annal.*, **69**, (1910), 331–371.
11. G. Hariharan, K. Kannan, A Comparison of Haar Wavelet and Adomian Decomposition Method for Solving One-dimensional Reaction-diffusion Equation, *International Journal of Applied Mathematics and Computation*, **2**(1), (2010), 50–61.

12. R. Hirota, Y. Ohta, Hierarchies of Coupled Soliton Equations, *International Journal of the Physical Society of Japan*, **60**, (1991), 798-809.
13. K. Khan, M. A. Akbar, Traveling Wave Solutions of Some Coupled Nonlinear Evolution Equations, *ISRN Mathematical Physics*, **2013**, (2013), 1-9.
14. N. A. Kudryashov, K. E. Shilnikov, A Note on The Tanh-coth Method Combined with the Riccati Equation for Solving Nonlinear Coupled Equation in Mathematical Physics, *Journal of King Saud University-Science*, **24**,(2012), 379-381.
15. Ü. Lepik, Application of Haar Wavelet Transform to Solving Integral and Differential Equations, *Proc. Estonian Acad. Sci. Phys. Math.*, **56(1)**, (2007), 28-46.
16. Ü. Lepik, Solving Differential and Integral Equations by Haar Wavelet Method, *Int. J. Math. Comput.*, **1**, (2008), 43-52.
17. A. Mohammadi, N. Aghazadeh, S. Rezapour, Haar Wavelet Collocation Method for Solving Singular and Nonlinear Fractional Time-dependent Emden-Fowler Equations with Initial and Boundary Conditions, *Mathematical Sciences*, **13**, (2019), 255-265.
18. A. Patra, S.S. Ray, Two-dimensional Haar Wavelet Collocation Method for the Solution of Stationary Neutron Transport Equation in a Homogeneous Isotropic Medium, *Ann. Nucl. Energy*, **70**, (2014), 30-35.
19. U. Saeed, M. Rehman, Haar Wavelet-quasilinearization Technique for Fractional Nonlinear Differential Equations, *Applied Mathematics and Computation*, **220**, (2013), 630-648.
20. I. Singh, S. Kumar, Haar Wavelet Methods for Numerical Solutions of Harry Dym (HD), BBM Burgers and 2D Diffusion Equations, *Bulletin Brazilian Mathematical Society*, **49(1)**, (2017), 1-26.
21. Siraj ul Islam, B. Sarler, I. Aziz, F. Haq, Haar Wavelet Collocation Method for the Numerical Solution of Boundary Layer Fluid Flow Problems, *Int. J. Therm. Sci.*, **50**, (2011), 686-697.
22. Siraj-ul-Islam, I. Aziz, A. S. Al-Fhaid, A. Shah, A Numerical Assessment of Parabolic Partial Differential Equations Using Haar and Legendre Wavelets, *Applied Mathematical Modelling*, **37**, (2013), 9455-9481.